Glycogen synthase kinase 3β/CCR6-positive bone marrow cells correlate with disease activity in multicentric Castleman disease-TAFRO

Nobuya Abe[1,2], Michihito Kono[1], Michihiro Kono[1,3], Naoki Ohnishi[1,3], Tomoya Sato[2], Masato Tarumi[1,2], Masaru Yoshimura[1], Taiki Sato[1], Kohei Karino[1], Yuka Shimizu[3], Yuichiro Fujieda[1], Masaru Kato[1], Rie Hasebe[4], Kenji Oku[1], Masaaki Murakami[2], and Tatsuya Atsumi[1]

[1]Department of Rheumatology, Endocrinology and Nephrology, Faculty of Medicine and Graduate School of Medicine, Hokkaido University, Sapporo, Japan. [2]Division of Molecular Psychoimmunology, Institute for Genetic Medicine, Graduate School of Medicine, Hokkaido University, Sapporo, Japan. [3]Third Department of Internal Medicine, Hokkaido P.W.F.A.C., Obihiro-Kosei General Hospital, Obihiro, Japan. [4]Biomedical Animal Research Laboratory, Institute for Genetic Medicine, Hokkaido University, Sapporo, Japan.

Running head: Disease-associated GSK3β^{+}CCR6^{+} cells in MCD-TAFRO

Corresponding author: Michihito Kono
Department of Rheumatology, Endocrinology and Nephrology, Faculty of Medicine, Hokkaido University, Kita 14, Nishi 5, Kita-ku, Sapporo, 060-8648, Japan
Email: m-kono@med.hokudai.ac.jp, Phone: +81-11-706-5915, Fax: +81-11-706-7710

Word counts: 3165

Summary

Multicentric Castleman disease–thrombocytopenia, anasarca, reticulin fibrosis of bone marrow, renal dysfunction and organomegaly (MCD-TAFRO) is an emergent phenotype characterized by lymphoproliferation, fluid collection, hemocytopenia, and multiple organopathy. Although studies have demonstrated an aberrant blood cytokine/chemokine profile referred to as “chemokine storm”, the pathogenesis remains unclear. We aimed to identify pathogenic key molecules, potential diagnostic targets and therapeutic markers in MCD-TAFRO using serum cytokine/chemokine profiles. We performed the targeted cytokine/chemokine multiplex analysis in six cases of MCD-TAFRO with remission or non-remission status. We observed significant changes in serum concentrations of CCL2, CCL5, and Chitinase-3-like-1 in the MCD-TAFRO patients with active state compared to inactive state. Ingenuity pathway analysis revealed that glycogen synthase kinase 3 (GSK3) and CCR6, which is expressed in megakaryocytes, were detected as upstream positive regulators for activating MCD-TAFRO status. More GSK3β+CCR6+ cells like megakaryocytes were detected in the bone marrow of patients with MCD-TAFRO than in those with systemic lupus erythematosus, MCD-not otherwise specified or autoimmune haemophagocytic lymphohistiocytosis. The cellularity of $GSK3\beta^{+}CCR6^{+}$ cells was correlated with disease activity, including thrombocytopenia and anaemia. In conclusion, GSK3β and CCR6 of bone marrow cells were potentially involved in the pathogenesis of MCD-TAFRO and may act as diagnostic targets and therapeutic markers.

Keyword

Multicentric Castleman disease-TAFRO; Lymphoproliferative disorders; Chemokine; Bone marrow; Glycogen synthase 3

Introduction

Multicentric Castleman disease (MCD) is one of the heterogeneous lymphoproliferative diseases, characterized by generalized lymphadenopathy with histopathologic features of hyaline vascular proliferation and plasma cell infiltration [1]. Among MCD cases, MCD-TAFRO is an emergent phenotype characterized by systemic inflammatory reaction with thrombocytopenia, anasarca, myelofibrosis, renal dysfunction, and organomegaly (TAFRO) [2]. The clinical symptoms of MCD-TAFRO are often more severe, leading to worse outcomes compared with the other subtype of MCD [3]. These clinical conditions and pathological findings overlap with a broad spectrum of other systemic autoimmune diseases. While the aetiology of MCD-TAFRO remains unclear, the proposed etiologic inducers of MCD pathogenesis include autoimmunity [1], autoinflammation [4], neoplasm and infection [5]. Thus, multiple immune dysregulations involving abnormal cytokine/chemokines profiles may promote MCD pathogenesis [6]. For example, hypercytokinaemia, including interleukin 6 (IL-6) and vascular endothelial growth factor (VEGF) [7,8] was proposed for the pathophysiology of MCD-TAFRO. The symptoms of capillary leak syndrome caused as adverse events of interleukin-2 (IL-2) immunotherapy overlap with MCD-TAFRO, suggesting the possible pathogenic contribution of IL-2 to MCD-TAFRO pathogenesis [9]. A previous proteomic analysis of six patients with MCD (2 MCD-TAFRO and 4 MCD-not other specified) revealed that multiple chemokine storms associated with MCD flares [10]. Therefore, analysing cytokine/chemokine profiles may be useful for clarifying the pathogenesis of MCD-TAFRO. Here, we report six cases of MCD-TAFRO where we conducted a multiplex cytokine/chemokine analysis to explore pathogenenic molecules, diagnostic targets and therapeutic markers.

Methods

Clinical information and evaluation of the patients included in this study

All the patients diagnosed via the 2015 proposed diagnostic criteria satisfied the 2019 updated diagnostic criteria [11,12] (detailed in Supplementary Methods). Cases 1, 2, 5 were diagnosed and managed in Hokkaido University Hospital, and cases 3,4,6 were in Obihiro-Kosei General Hospital. As a previous report described, active/non-remission disease including disease relapse was defined by hypoalbuminemia (< 3.5 g/dL), elevated levels of C-reactive protein (CRP) (> 10 mg/L), anaemia (haemoglobin < 13.5 g/dL), renal insufficiency (creatinine > 1.3 mg/dL), constitutional symptoms, and/or fluid collection in body cavities [13]. Inactive/remission disease was defined as the absence of any of these symptoms. Disease severity classification scoring was based on the degree of present symptoms including anasarca, thrombocytopenia, fever and/or inflammation and renal insufficiency respectively scored from 0 to 3. Relationship between the score and disease severity was defined as following: 0–4 points, mild disease (Grade 1); 5–6 points, moderate disease (Grade 2), 7–8 points, slightly severe disease (Grade 3); 9–10 points, severe disease (Grade 4); 11–12 points, very severe disease (Grade 5) [12]. Therapeutic response was assessed regarding the NCI-CTCAE ((National Cancer Institute-Common Terminology Criteria for Adverse Events) version 4.0 about 34 MCD-related symptoms and signs [14]. Therapeutic approach was initially started using glucocorticoids (1.0 mg/kg/day) including methylprednisolone pulse therapy (500-1000 mg of methylprednisolone for 3 consecutive days). When the patients were unresponsive to the initial treatment, different treatments such as cyclosporine, tacrolimus, tocilizumab, rituximab, intravenous immunoglobulin (IVIg) and thrombopoietin receptor agonist (TPORA) was applied at attending physician’s discretion. Supportive cares including blood transfusion, haemodialysis, plasmapheresis and mechanical ventilation were applied properly. Bone marrow in the patients with MCD-TAFRO were biopsied with Original Jamshidi™ (Becton, Dickinson and Company, Franklin Lakes, NJ, USA) in

active and inactive disease status. The lymph node specimens were surgically resected for the diagnosis in a clinical setting. At patient's baseline data, interleukin-6 (IL-6) and vascular endothelial growth factor (VEGF) were measured by enzyme immunoassay in clinical laboratory using Human IL-6 QuantiGlo ELISA Kit and Human VEGF Quantikine ELISA Kit (R&D Systems), and their lower limit of reference range were 4.0 pg/mL and 38.3 pg/mL, respectively. Also, serum levels of glycogen synthetase kinase (GSK) 3β and CC chemokine receptor (CCR) 6 were evaluated using Glycogen Synthase Kinase 3 β ELISA Kit (Cloud-clone corp.) and Human CCR6 ELISA Kit (Aviva Systems Biology).

For comparison, we extracted the serum and bone marrow specimens of treatment-naïve patients with systemic lupus erythematosus (SLE) (n = 4 sera and 5 bone marrows), MCD-not otherwise specified (MCD-NOS) (n = 2 sera and 3 bone marrows) and autoimmune haemophagocytic lymphohistiocytosis (HLH) (n = 4 sera and 5 bone marrows) diagnosed and managed in Hokkaido University Hospital. The patients with SLE manifested pancytopenia or thrombocytopenia without hemophagocytosis. The patients with autoimmune HLH complicated with mixed connective tissue disease (MCTD), adult-onset Still's disease (AOSD), SLE and dermatomyositis (DM).

Ethical approval of conducting the present study was obtained from Institutional Review Board of Hokkaido University Hospital (reference number: 020-0042). This study complied with the Declaration of Helsinki. We obtained the patient informed consents for participation in this study and publication from all the patients included in this study.

Cytokine/chemokine multiplex analysis

We performed multiplex cytokine/chemokine beads assays using sera of the patients and a Luminex® Assay and a Luminex® High Performance Assay (LXSAHM and FCSTM, R&D Systems, Minneapolis, MN, United States of America) analysed with a Luminex® 200 xPONENT® System (Merck KGaA, Darmstadt, Germany) in accordance with the

manufacturer's protocols in the laboratory of Institute for Genetic Medicine, Hokkaido University. The measured analytes of cytokines and chemokines included tumour necrosis factor α (TNFα), interferon (IFN)-γ, IL-1β, IL-2, IL-4, IL-5, IL-6, IL-8/C-X-C motif chemokine ligand (CXCL) 8, IL-10, IL12p70, IL-13, IL-17, IL-18, IL-23, IL-1 receptor-like 1/ST2, CXCL1/Growth-related oncogene α, CXCL13/B lymphocyte chemoattractant, C-C motif chemokine ligand (CCL) 2/monocyte chemotactic protein-1 (MCP-1), CCL3/macrophage inflammatory protein-1α (MIP-1α), CCL5/Regulated on Activation, Normal T cell Expressed and Secreted (RANTES), CCL7/MCP3, CCL20/MIP-3, TNF ligand superfamily member 13 (TNFSF13)/A proliferation-inducing ligand (APRIL), TNFSF13B/B cell activating factor belonging to the TNF family (BAFF), Chitinase-3-like-1 (CHI3L1), epidermal growth factor, fibroblast growth factor 23 (FGF-23), and VEGF-A. The sera of the patients with MCD-TAFRO were collected at initial onset, remission, or relapse, and during receiving ineffective treatment. The collected sera were centrifuged at 3000 rotations per minute at 4 °C for 15 minutes, and the supernatant was stored at -80 °C until use.

Proteomic analysis

The serum cytokines and chemokines data at active disease phase and inactive disease phase were subjected to protein-protein interaction (PPI) analysis using The Search Tool for the Retrieval of Interacting Genes (STRING) database [15]. By Ingenuity Pathway Analysis (IPA) (QIAGEN, Hilden, Germany), upstream regulator analysis, disease/toxic functional analysis and regulatory effect analysis were performed using serum cytokines and chemokines data with differential abundance between a phase of active and inactive disease.

Immunohistochemistry

We used the healthy volunteer's specimens of bone marrow (Human bone marrow Paraffin Tissue Section, HP-704, Zyagen) as a healthy control.

The specimens were fixed in 4% paraformaldehyde, embedded in paraffin, and sectioned at 5-10 μm. The sections were deparaffinized with xylene and dehydrated with ethanol. Heat-induced antigen retrieval was performed with citrate sodium. The sections were rinsed with TBS-0.1% Tween and blocked with 5% BSA and 0.3% Triton X-100 in PBS for 1h. Primary antibodies were diluted in antibody buffer containing as 2% BSA and 0.3% Triton X-100 as follows: Rabbit anti-human GSK 3β (1:100, HPA028017, Sigma-Aldrich), Rat anti-human CCR 6 (1:200, clone: 18B9E6, Novus biologicals), Mouse anti-human CD61 (1:25, clone: VI-PL2, LSBio) and Mouse anti-human CD163 (1:50, clone: EDHu-1, Novus Biologicals), and incubated overnight at 4 °C. Secondary Alexa-conjugated antibodies (Invitrogen) were added at 1:200 in the antibody buffer for 2 h at room temperature. Slides were mounted in ProLong™ Diamond Antifade Mountant with DAPI (ThermoFisher Scientific) and imaged using the Keyence inverted fluorescence microscope, BZ-9000 (Keyence Japan, Osaka, Japan). All quantifying analyses for fluorescent positive cells were performed by a blinded observer (Tomoya S) to the patients' clinical data using Image J software (National Institutes of Health, Bethesda, Maryland, USA). We performed correlation analyses using the results of the quantification and clinical data.

Statistical analysis

We used analysis of variance (ANOVA) to compare the values of unpaired continuous variables with groups. For multiple comparisons, we applied Holm-Sidak's method. Wilcoxon signed-rank test was used for paired comparisons of continuous variables. Correlations were determined using Pearson's product-moment correlation coefficient. We used JMP® Pro 13 software (SAS Institute Inc., Cary, NC, USA) and GraphPad Prism® version 7.04 (GraphPad Software, San Diego, CA, USA) for statistical analyses.

When the p-value was below 0.05, the results were defined as statistically significant. All statistical tests were two-sided.

Results

Significant changes of serum cytokines and chemokines

Clinical information and treatment courses of six MCD-TAFRO patients (cases 1-6) are summarized in Table 1, Supplementary Methods and Fig. S1. To elucidate the pathogenesis, diagnostic targes and therapeutic markers for MCD-TAFRO, we performed a multiplex cytokine/chemokine analysis using the MCD-TAFRO patients' sera in this case series. A total of the 20 samples were analysed and three were collected in initial onset without treatment and six in remission under cyclosporine A (CsA) therapy except the case 6 under tocilizumab treatment (Fig. 1A, B). The multiplex analysis results were as follows; there were no samples in which IL-17 and IL-23 were detected. The average serum values of ILs had absence of the trend among each case regardless of the disease activity status (Table S1). Meanwhile, the changes in the levels of some analytes including IL1RL1/ST2, CCL2/MCP-1, CCL3/MIP-1α, CCL5/RANTES, CCL7/MCP-3, CCL20/MIP-3, TNFSF13/APRIL, CHI3L1 and FGF-23 showed a pattern between the remission state and the non-remission state (Fig. 1C). Among these, the average levels of CCL2/MCP-1, CCL5/RANETS significantly increased in the remission compared with the non-remission, and CHI3L1 significantly decreased after remission. Indeed, the serum levels of CCL2/MCP-1 and CCL5/RANTES were elevated the most during remission in all the cases. Also, serum FGF-23 levels were most decreased in the remission state of all the patients (Fig. S2A-F). Thus, the serum levels of some chemokines and growth factors were definitely affected by treatment and disease activity status, possibly becoming new therapeutic biomarker in MCD-TAFRO.

Predicted activation of glycogen synthase kinase 3β and CCR6 in non-remission state of MCD-TAFRO

Next, we performed a PPI analysis using the ratio of average serum levels of multiplexed cytokines and chemokines in non-remission state of MCD-TAFRO to those in remission.

PPI network for the cytokines and chemokines showed some sort of connection with each analyte (Fig. 2A). The upstream regulator analysis demonstrated that 21 molecules were predicted as significant upstream activators or inhibitors with Z-score >2.0 in non-remission stated MCD-TAFRO. The predicted upstream activators with high activation Z-score (>2.0) included CCR6 and GSK3 (Fig. 2B). RIPK1, SMAD3, CTNNB1, IL20RB, EGR1 and EGR2 were included as the predicted upstream inactivators with low activation Z-score (<2.0) in non-remission MCD-TAFRO. The disease and toxic function analysis predicted the significant inhibition of leucocytosis, haematopoiesis and antigen presenting cells development, and the increased probability of developing glomerulonephritis (Fig. 2C, D). Regulatory effect analysis revealed that the predicted states of the regulators including EGR2, GSK3, IL20RB and EGR1 were consistent with the measured status of target molecules in dataset such as CCL2/MCP-1, CCL5/RANTES, IL-8/CXCL8, TNF-α and VEGF-A, and were expected to have impacts on diseases and functions such as development of phagocytes, glomerulonephritis, leucocytosis and development of antigen presenting cells (Fig. S3). Thus, proteomic analysis using serum multiplex cytokine/chemokine level would lead the candidates related to the disease activity of MCD-TAFRO.

Highly expressed GSK3β and CCR6 in bone marrow of MCD-TAFRO, correlating with systemic inflammation

We evaluated the protein expression of GSK and CCR6 in bone marrow and lymph node of the patients with MCD-TAFRO and a healthy control via immunohistochemistry. Human GSK3 has two isoforms, α and β, and The Human Protein Atlas (available from https://www.proteinatlas.org/) [16], a public protein database, demonstrated that GSK3α highly expresses even in bone marrow and lymph node of healthy human, but not GSK3β (Fig. S4A). Previous reports demonstrated GSK3β as a regulator of megakaryocytic

differentiation and platelet production in bone marrow [17,18]. Therefore, we assessed the expression of GSK3β isoform.

We identified GSK3β and CCR6-positive cells in bone marrow of MCD-TAFRO patients while these cells were not detected in the healthy control. These GSK3β/CCR6-double positive cells included relatively large cells and a part of cells were multinucleid, which suggest these cells are megakaryocytes. Compared to effectively treated state of MCD-TAFRO, GSK3β or CCR6-positive cells, and GSK3β/CCR6-double positive cells were significantly increased in untreated or ineffectively treated state (Fig. 3A and Fig. S4B). Next, we investigated the nature of these cells using immunostatinig of CD61 and CD163, which are cell markers for megakaryocytes and monocytes/macrophages, respectively. In the bone marrows of patients with MCD-TAFRO, a part of GSK3β/CCR6-double positive cells were colocalized with CD61, but not CD163 (Fig. 4B), suggesting that the cells were of the megakaryocyte lineage. Furthermore, the percentage of GSK3β/CCR6-double positive cells was correlated with disease grade of MCD-TAFRO, platelet count and haemoglobin level, but not serum CRP level (Fig. 3C and Fig. S4D). Regarding 34 MCD-related symptoms and signs evaluated by NCI-CTCAE (National Cancer Institute-Common Terminology Criteria for Adverse Events) version 4.0 (Table S2)[14], the cellularity of GSK3β/CCR6-double positive cells in bone marrow of the patients with MCD-TAFRO was significantly correlated with the grades of the symptoms and signs such as fatigue, dyspnoea, generalized oedema and the total score (Fig. S4D). Ascites was tended to correlate, but the symptoms including fever and pleural effusion had no significant correlation with GSK3β/CCR6-double positive cells (Fig. 3C and Fig. S4D). Comparing with disease controls such as SLE without HLH and MCD-NOS, $GSK3\beta^{+}CCR6^{+}$ cells were detected specifically in treatment-naïve patients with MCD-TAFRO (Fig. 4D). Although haemophagocytosis was not observed in bone marrows of the MCD-TAFRO patients, we investigated the effect of inflammation for these cells using bone marrow samples of patients with autoimmune HLH.

GSK3β^{+}CCR6^{+} cells were also detected in autoimmune HLH secondary to MCTD, AOSD, SLE and DM, but the percentage of these cells in the bone marrow was less than those with treatment-naïve MCD-TAFRO (Fig. 4D).

We finally measured serum levels of GSK3β and CCR6 in MCD-TAFRO and the other diseases including MCD-NOS, SLE and autoimmune HLH. No GSK3β was detected in all the serum samples of our study. Serum CCR6 level of MCD-TAFRO was not elevated compared with the other diseases (Fig. S4E), suggesting that the GSK3β/CCR6-double positive cells were specifically regulated in bone marrows of MCD-TAFRO.

Thus, the GSK3β/CCR6-double positive cells in bone marrow would be involved in the pathogenesis of MCD-TAFRO, a novel diagnostic target and a therapeutic marker in MCD-TAFRO.

Discussion

We investigated the transition of serum cytokine/chemokine levels based on MCD-TAFRO case series to evaluate novel molecules for the pathogenesis. This study revealed that the levels of chemokines and growth factors such as CCL2/MCP-1, CCL5/RANETS and CHI3L1 were significantly changed by treatment in MCD-TAFRO. GSK3β and CCR6, which were predicted as the upstream activators, were highly and specifically expressed in the bone marrow of active MCD-TAFRO, positively correlating with its disease activity and laboratory findings associated with thrombocytopenia and anaemia.

There are a few studies exploring the pathogenesis and therapeutic approaches of MCD-TAFRO from the aspect of proteome. The first report using flowcytometry-based multiplex assay from Japan revealed that the serum CXCL10 level of MCD-TAFRO was significantly higher than that of MCD-NOS and healthy controls [19]. Also, a high-throughput protein quantifying analysis demonstrated that multiple chemokines including CXCL13, CCL21 and CCL23 were significantly high level during MCD-TAFRO flare compared with the remission state [10]. Our study could not demonstrate the elevated level of serum CXCL13 in non-remission MCD-TAFRO. However, the levels of multiple chemokines including CCL2/MCP-1, CCL3/MIP-1α, CCL5/RANTES, CCL7/MCP-3 and CCL20/MIP-3 had a certain tendency between remission state and non-remission state. Surprisingly, CCL2/MCP-1 and CCL5/RANTES levels were elevated via successful treatment using CsA or tocilizumab. Thus, the dysregulation of chemokines could have a prominent role for developing the pathogenesis of MCD-TAFRO.

Our analysis demonstrated GSK3β and CCR6 as the candidates of positive regulators in MCD-TAFRO. CCR6 is a CC chemokine receptor protein and its ligand is CCL20/MIP-3α. CCR6 is expressed on various immune cells including T cells, B cells, dendric cells, NK cells and even bone marrow megakaryocytes. Megakaryocytes express several

chemokine receptors including CXCR4, CCR6, CCR8, CCR5 and CCR2 [20]. Indeed, our immunohistochemical findings showed that CCR6-positive cells in bone marrows are relatively large and multinucleid, suggesting CCR6-positive megakaryocytes. Furthermore, a part of these cells expressed CD61, a cell surface marker of megakaryocytes, suggesting that the cells are of megakaryocyte lineage. However, the function of CCR6 signalling in megakaryocytes remains to be established.

On the other hand, GSK3 is a serine/threonine kinase and the phosphorylation permits many biological activities such as glycogen metabolism, cell signalling and cellular transport [21]. GSK3β, one of the GSK isoforms, is reportedly associated with a variety of diseases such as diabetes, malignancy, inflammatory disorders, Alzheimer's disease. The present study demonstrated that the percentage of GSK3β/CCR6-double positive cells in bone marrow, which was assumed to be megakaryocytes, was correlated with platelet counts and haemoglobin level. Previous reports revealed that GSK3β inhibition promotes megakaryocytic survival and proliferation by thrombopoietin-induced Akt signalling [17], and thrombopoiesis from megakaryocytes [18]. Moreover, in our study, we focused on GSK3β/CCR6-double positive cells in bone marrow. Taken together, these cells would be megakaryocytes with impaired cell function such as proliferation and platelet production. Furthermore, GSK3β negatively regulates CCL5/RANTES production from inflammatory cells and this chemokine increases proplatelet formation of megakaryocytes [22,23]. Not limited to hematopoietic cells, previous proteomic research also revealed activated $CD8^+$ T cells and PI3K/Akt/mTOR signalling activation in IL-6 inhibitor-resistant MCD-TAFRO with active disease [13], also indicating the association of GSK3β signalling. Moreover, GSK3β facilitates pathogenic Th17 polarization and inhibition of GSK3β promotes the polarization of regulatory T cells [24-28]. GSK3β also inhibits IL-8 production [29], which is compatible with our results of decreasing IL-8 signalling in MCD-TAFRO with non-remission state.

In this study, the patients with autoimmune HLH had GSK3β/CCR6-double positive cells in the bone marrow. Especially, SLE-HLH patients demonstrated higher percentage of GSK3β/CCR6-double positive cells, indicating that inflammatory process induced these cells to some degree. Indeed, patients with SLE showed clinical manifestations such as thrombocytopenia, serositis, fever and splenomegaly similar to those in MCD-TAFRO [30]. It is thus biologically plausible that specific pathological environment called chemokine storm is associated with the development of MCD-TAFRO, and it would not merely impair hematopoietic cells like megakaryocyte in bone marrow, but also affect various cells in multiple organs, leading to a variety of clinical manifestations. GSK3β signalling pathway would be unitarily associated with some parts of the pathogenesis in MCD-TAFRO.

We acknowledge several limitations in this study. Because this study is case series analysis, the number of patients was small. Targeted multiplex cytokines/chemokines assay would also produce biased interpretation of the results. Although all the case except one achieved remission by CsA treatment, heterogeneous therapeutic regimen may impact the cytokine/chemokine profiles. However, under this circumstance, there were the tendencies for the transition of some chemokines' concentrations and immunohistochemical findings corresponding to remission or non-remission status. We believe that our preliminary results would be worth further analysing for verification.

In conclusion, proteomic analysis using multiplex serum cytokine/chemokine results detected GSK3β and CCR6 as upstream positive regulators in MCD-TAFRO with active disease. The cellularity of GSK3β/CCR6-double positive cells in bone marrow correlated with disease severity of MCD-TAFRO. Although further functional research for the

MCD-TAFRO pathogenesis was required, GSK3β and CCR6 would be a diagnostic molecules and novel therapeutic targets of MCD-TAFRO.

Acknowledgements

We thank the physicians and technicians from Department of Surgical pathology, Hokkaido University Hospital and from Department of Clinical Pathology, Hokkaido P.W.F.A.C., Obihiro-Kosei General Hospital for pathological diagnosis and sample processing, and clinical laboratory technicians from Division of Laboratory and Transfusion Medicine, Hokkaido University Hospital for clinical flowcytometric analysis. We thank Mses. Yumiko Kaneko, Yui Ishikura, and Chiemi Nakayama for their technical support, and Mses. Shikishi Chida and Satomi Fukumoto for their secretary support.

Author contributions

NA conducted data analyses, contributed to study design, clinical data, sample collection and writing the manuscript. Michihito K contributed to study design, data interpretation, and writing the manuscript. Michihiro K and NO contributed to clinical data and sample collection. Tomoya S contributed to data analysis. MY, Taiki S, KK, YS, YF, Masaru K and KO contributed to clinical data and sample collection. RH and MM contributed to data collection and analysis. TA contributed to clinical data, data interpretation and writing the manuscript.

Conflict of interest

None declared.

Supporting information

Additional supporting information may be found online inthe Supporting Information section at the end of the article.

Supplementary Methods

Fig S1. Clinical course and relevant data of a multicentric Castleman disease-TAFRO cases in this study.

Fig S2. Changes of the serum cytokine and chemokine levels in the clinical course of the patients with MCD-TAFRO.

Fig S3. Regulator effects analysis of the predicted upstream regulators in Ingenuity Pathway Analysis.

Fig S4. Additional images of immunohistochemistry with the correlation analyses between the quantifying result of immunohistochemistry and clinical data.

Table S1. Multiplex cytokines/chemokines analysis results in the six MCD-TAFRO patients.

Table S2. Multicentric Castleman's disease signs and symptoms by NCI-CTCAE, version 4.0

REFERENCES

1. Liu AY, Nabel CS, Finkelman BS, et al. Idiopathic multicentric Castleman's disease: a systematic literature review. *Lancet Haematol.* 2016;**3**:e163-75.
2. Fajgenbaum DC, Uldrick TS, Bagg A, et al. International, evidence-based consensus diagnostic criteria for HHV-8-negative/idiopathic multicentric Castleman disease. *Blood.* 2017;**129**:1646-57.
3. Iwaki N, Fajgenbaum DC, Nabel CS, et al. Clinicopathologic analysis of TAFRO syndrome demonstrates a distinct subtype of HHV-8-negative multicentric Castleman disease. *Am J Hematol.* 2016;**91**:220-6.
4. Kone-Paut I, Hentgen V, Guillaume-Czitrom S, Compeyrot-Lacassagne S, Tran TA, Touitou I. The clinical spectrum of 94 patients carrying a single mutated MEFV allele. *Rheumatology (Oxford).* 2009;**48**:840-2.

5. You L, Lin Q, Zhao J, Shi F, Young KH, Qian W. Whole-exome sequencing identifies novel somatic alterations associated with outcomes in idiopathic multicentric Castleman disease. *Br J Haematol.* 2019.
6. Fajgenbaum DC. Novel insights and therapeutic approaches in idiopathic multicentric Castleman disease. *Blood.* 2018;**132**:2323-30.
7. Yoshizaki K, Matsuda T, Nishimoto N, et al. Pathogenic significance of interleukin-6 (IL-6/BSF-2) in Castleman's disease. *Blood.* 1989;**74**:1360-7.
8. Leger-Ravet MB, Peuchmaur M, Devergne O, et al. Interleukin-6 gene expression in Castleman's disease. *Blood.* 1991;**78**:2923-30.
9. Konishi Y, Takahashi S, Nishi K, et al. Successful Treatment of TAFRO Syndrome, a Variant of Multicentric Castleman's Disease, with Cyclosporine A: Possible Pathogenetic Contribution of Interleukin-2. *Tohoku J Exp Med.* 2015;**236**:289-95.
10. Pierson SK, Stonestrom AJ, Shilling D, et al. Plasma proteomics identifies a 'chemokine storm' in idiopathic multicentric Castleman disease. *Am J Hematol.* 2018;**93**:902-12.
11. Masaki Y, Kawabata H, Takai K, et al. Proposed diagnostic criteria, disease severity classification and treatment strategy for TAFRO syndrome, 2015 version. *Int J Hematol.* 2016;**103**:686-92.
12. Masaki Y, Kawabata H, Takai K, et al. 2019 Updated diagnostic criteria and disease severity classification for TAFRO syndrome. *Int J Hematol.* 2020;**111**:155-8.
13. Fajgenbaum DC, Langan RA, Japp AS, et al. Identifying and targeting pathogenic PI3K/AKT/mTOR signaling in IL-6-blockade-refractory idiopathic multicentric Castleman disease. *J Clin Invest.* 2019;**130**:4451-63.

14. van Rhee F, Wong RS, Munshi N, et al. Siltuximab for multicentric Castleman's disease: a randomised, double-blind, placebo-controlled trial. *Lancet Oncol.* 2014;**15**:966-74.
15. Franceschini A, Szklarczyk D, Frankild S, et al. STRING v9.1: protein-protein interaction networks, with increased coverage and integration. *Nucleic Acids Res.* 2013;**41**:D808-15.
16. Uhlén M, Fagerberg L, Hallström BM, et al. Proteomics. Tissue-based map of the human proteome. *Science.* 2015;**347**:1260419.
17. Soda M, Willert K, Kaushansky K, Geddis AE. Inhibition of GSK-3beta promotes survival and proliferation of megakaryocytic cells through a beta-catenin-independent pathway. *Cell Signal.* 2008;**20**:2317-23.
18. Ono M, Matsubara Y, Shibano T, Ikeda Y, Murata M. GSK-3β negatively regulates megakaryocyte differentiation and platelet production from primary human bone marrow cells in vitro. *Platelets.* 2011;**22**:196-203.
19. Iwaki N, Gion Y, Kondo E, et al. Elevated serum interferon γ-induced protein 10 kDa is associated with TAFRO syndrome. *Sci Rep.* 2017;**7**:42316.
20. Majka M, Ratajczak J, Baj-Krzyworzek M, et al. Biological significance of chemokine receptor expression by normal human megakaryoblasts. *Folia Histochem Cytobiol.* 2001;**39**:235-44.
21. Jope RS, Johnson GV. The glamour and gloom of glycogen synthase kinase-3. *Trends Biochem Sci.* 2004;**29**:95-102.
22. Huang WC, Lin YS, Wang CY, et al. Glycogen synthase kinase-3 negatively regulates anti-inflammatory interleukin-10 for lipopolysaccharide-induced iNOS/NO biosynthesis and RANTES production in microglial cells. *Immunology.* 2009;**128**:e275-86.
23. Machlus KR, Johnson KE, Kulenthirarajan R, et al. CCL5 derived from platelets increases megakaryocyte proplatelet formation. *Blood.* 2016;**127**:921-6.

24. Beurel E, Yeh WI, Michalek SM, Harrington LE, Jope RS. Glycogen synthase kinase-3 is an early determinant in the differentiation of pathogenic Th17 cells. *J Immunol.* 2011;**186**:1391-8.
25. Beurel E, Kaidanovich-Beilin O, Yeh WI, et al. Regulation of Th1 cells and experimental autoimmune encephalomyelitis by glycogen synthase kinase-3. *J Immunol.* 2013;**190**:5000-11.
26. Patterson AR, Endale M, Lampe K, et al. Gimap5-dependent inactivation of GSK3β is required for CD4(+) T cell homeostasis and prevention of immune pathology. *Nat Commun.* 2018;**9**:430.
27. Han D, Medina-Rodriguez EM, Lowell JA, Beurel E. Glycogen synthase kinase-3 promotes T helper type 17 differentiation by promoting interleukin-9 production. *Immunology.* 2020;**160**:357-65.
28. Ding Y, Shen S, Lino AC, Curotto de Lafaille MA, Lafaille JJ. Beta-catenin stabilization extends regulatory T cell survival and induces anergy in nonregulatory T cells. *Nat Med.* 2008;**14**:162-9.
29. Wang Q, Zhou Y, Wang X, Evers BM. Glycogen synthase kinase-3 is a negative regulator of extracellular signal-regulated kinase. *Oncogene.* 2006;**25**:43-50.
30. Kaul A, Gordon C, Crow MK, et al. Systemic lupus erythematosus. *Nat Rev Dis Primers.* 2016;**2**:16039.

FIGURE LEGENDS

Fig. 1. **Multiplex cytokine/chemokine analysis of the MCD-TAFRO patients**

(**A**) Schema of the disease state and therapeutic approaches at the time of blood collection. Thick vertical arrow indicates the timing of blood collection. The disease state is described above the horizontal thin arrow of timeline and the details of therapeutic agents are described below. Clinical courses on solid timeline are shown in the present study, but those on dashed timeline are not. (**B**) Shema of multiplex cytokine/chemokine analysis using collected sera from the MCD-TAFRO patients and described 28 analytes. (**C**) Paired individual trajectories of change in serum cytokine/chemokine levels between non-remission state and remission state of the MCD-TAFRO patients ($n = 6$). *$p < 0.05$, Wilcoxon signed-rank test was used for paired comparisons.

Abbreviations: CsA, cyclosporine A; IVIg, intravenous immunoglobulin; MMF, mycophenolate mofetil; mPSL, methylprednisolone; PSL, prednisolone; RTX, rituximab; TAC, tacrolimus, TCZ, tocilizumab.

Fig. 2. **Proteomic analysis using the results of multiplex cytokine/chemokine data of the MCD-TAFRO patients**

(**A**) Protein-protein interaction network using the ratio of average serum cytokine/chemokine concentration in non-remission state to remission state of MCD-TAFRO patients, constructed by STRING (Search Tool for the Retrieval of Interacting Genes) database version 11.0. Edges represent protein-protein associations corresponding to its colouring described in the legend. The halo colour is based on the rank of the protein in the full set of input values. Red halo shows the high rank, blue halo shows the low rank, and grey halo shows the other medium rank. (**B**-**D**) Volcano plot displaying (**B**) predicted upstream regulators, (**C**) associated diseases and functions, and (**D**) predicted toxic function by IPA for the non-remission state to the remission state. The vertical axis (y-axis) corresponds to the value of log 10 (p-value), and the horizontal

axis (x-axis) displays the activation Z-score. The red dots represent the predictably activated items; the blue dots represent the inhibited items. Positive x-values represent predictably activated and negative x-values represent predictably inhibited. Orange horizontal line denotes p-value of 0.05 (prior to logarithmic transformation), a significant threshold.

Fig. 3. **Expression of glycogen synthase kinase 3β and CCR6 in bone marrow of the MCD-TAFRO patients, correlating with disease activity and laboratory findings** (**A**) Immunohistochemical images of bone marrow overlaid with glycogen synthase kinase 3β (GSK3β, magenta) and CCR6 (green). The magnified panel shows the area which arrow indicates. Scale bars, 50 μm. The percentages of GSK3β-positive cells, CCR6-positive cells and GSK3β/CCR6-double-positive cells in bone marrow of MCD-TAFRO with remission state (n = 2), MCD-TAFRO with non-remission (n = 7), a healthy control are quantified and shown graphically. Data are mean ± s.e.m. (**B**) Representative immunohistorical images in colocalization analysis of GSK3β/CCR6-double-positive cells with CD61 and CD163 (red) in MCD-TAFRO patients. The magnified panel with separated colours shows the area which arrow indicates. Scale bars, 50 μm. (**C**) Correlations between GSK3β/CCR6-double-positive cells in bone marrow of MCD-TAFRO patients and their clinical data. Dot plot shows individual cases and blue colour indicates the patient with remission state; red with non-remission state. Statistical analysis was performed by Pearson's product-moment correlation coefficient. (**D**) Representative immunohistochemical images of bone marrow in patients with MCD-NOS (n = 3), systemic lupus erythematosus (SLE) (n = 5) and autoimmune haemophagocytic lymphohistiocytosis (HLH) secondary to mixed connective tissue disease (MCTD), adult-onset Still's disease (AOSD), dermatomyositis (DM) and SLE for GSK3β and CCR6. *$p < 0.05$, ****$p < 0.0001$, ANOVA with post-hoc Holm-Sidak

method. Scale bar, 50 μm. Small panel represents the area indicated by arrows. Data are mean ± s.e.m.

542 **TABLES**

Table 1. Characteristics and disease/treatment history at disease new-onset or flare for MCD-TAFRO 1-6 patients

Patient number of MCD-TAFRO	1	2	3	4	5	6
Demographics and diagnosis						
Disease new-onset or flare	New	New	Flare	Flare	New	New
Sex	F	F	M	F	F	F
Age at disease onset or flare	43	47	64	67	62	66
Multicentric lymphadenopathy	+	+	+	+	+	+
Lymph node pathology	N.D.	N.D.	N.D.	Mixed variant subtype	Hypervascular subtype	N.D.
Bone marrow pathology	Reticulin myelofibrosis Increased number of megakaryocytes with slight hyperplasia	Reticulin myelofibrosis Increased number of megakaryocytes with slight hyperplasia	Reticulin myelofibrosis Increased number of megakaryocytes	N.D.	N.D.	No specific findings
Disease severity grade	3	4	2	2	3	3
Clinical characteristics and laboratory findings [reference range] at disease onset or flare						
Fever	+	+	-	-	+	+
Oedema	+	+	+	+	+	+
Anasarca	+	+	+	+	+	+
Organomegaly	+	+	+	+	+	+
Haemoglobin (g/dL) [11.6-14.8]	8.4	6.8	9.9	13.6	11.8	9
Platelet count ($\times 10^4/\mu L$) [15.8-34.8]	4.4	3.9	5.2	7.2	6.4	2.5
Albumin (g/dL) [4.1-5.1]	1.3	2.6	3.2	3.5	4.0	2.1

Immunoglobulin G (mg/dL) [861-1747]	1631	1336	540	650	2269	1588
Immunoglobulin G4 (mg/dL) [4-108]	48	60.1	N.D.	16.6	266	34.9
Creatinine (mg/dL) [0.46-0.79]	1.14	1.00	1.37	1.26	0.83	1.10
Haematuria	-	+	2+	-	+	+
Proteinuria (g/g･Cr)	2.17	3.74	0.40	0.18	5.61	0.92
Alkaline phosphatase (U/L) [106-322]	432	347	168	188	529	334
C-reactive protein (mg/L) [<1.4]	185.8	55.6	28.2	11.2	2.3	107
Procalcitonin (ng/mL) [<0.50]	5.07	1.81	0.82	1.3	N.D.	2.72
Soluble interleukin-2 receptor (U/mL) [<459]	1691	659	1070	1889	812	834
Interleukin-6 (pg/mL) [< 4.0]	8.4	25	6.8	48.1	N.D.	86.1
Vascular endothelial growth factor (pg/mL) [< 38.3]	253	118	208	357	N.D.	981
Rheumatoid factor (IU/mL) [<15]	11.7	16.6	-	3	-	77
Complement 3 (mg/dL) [73-138]	94	115	88	107	101	103
Complement 4 (mg/dL) [11-31]	26	24	22	48.1	27	18
50% hemolytic complement activity (U/mL) [31.6-57.6]	54.1	78.7	60	23	62	60
Antinuclear antibody	1:1280 (Speckled, Cytoplasmic)	1:1280 (Speckled)	1:40 (Speckled)	1:80 (Homogeneous, Speckled)	1:320 (Homogeneous,	1:80 (Speckled)

					Speckled, Nucleolar)	
Disease-specific autoantibodies	anti-Ro (132.3 U/mL) anti-La (48.4 U/mL) anti-thyroperoxidase (11.47 U/mL) anti-mitochondria M2 (132 Unit) Lupus anticoagulant (1.41)	anti-U1-RNP (178.3 U/mL) anti-thyroglobulin (2757.23 U/mL) anti-thyroperoxidase (732.58 U/mL) Lupus anticoagulant (1.27)	-	anti-Ro (129.4 U/mL) anti-La (31.0 U/mL)	-	anti-double stranded DNA (21.4 U/mL) anti-Ro (101.0 U/mL)
Treatment history						
Pretreatment	N.A.	N.A.	PSL 10 mg/day	PSL 12.5 mg/day, TAC	N.A.	N.A.
Experienced treatment	N.A.	N.A.	PSL	mPSLpulse, PSL, TAC, RTX, TCZ	N.A.	N.A.
Therapeutic agents for initial onset or flare	mPSLpulse, PSL, TCZ, RTX, CsA	mPSLpulse, PSL, MMF, TAC, TCZ, CsA	mPSLpulse, PSL dose-increase, TAC, IVIg, CsA	PSL dose-increase, RTX, CsA, IVIg	PSL, CsA	mPSLpulse, PSL, Intravenous CsA, IVIg, TCZ
Treatment efficacy	+	+	+	+	+	+
Effective agents	CsA	CsA	CsA	CsA, IVIg	PSL, CsA	TCZ
Adverse events	-	-	-	-	-	+, CsA-induced thrombotic microangiopathy

543 Abbreviations: CsA, cyclosporine A; IVIg, intravenous immunoglobulin; MMF, mycophenolate mofetil; mPSL, methylprednisolone;

544 PSL, prednisolone; RTX, rituximab; TAC, tacrolimus, TCZ, tocilizumab.

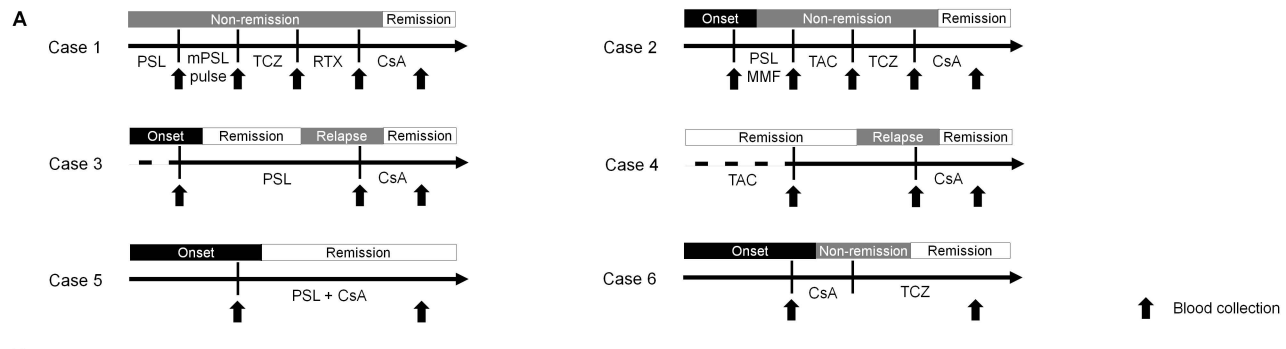
A
Case 1
Non-remission
Remission
PSL
mPSL pulse
TCZ
RTX
CsA
Case 2
Onset
Non-remission
Remission
PSL MMF
TAC
TCZ
CsA
Case 3
Onset
Remission
Relapse
Remission
PSL
CsA
Case 4
Remission
Relapse
Remission
TAC
CsA
Case 5
Onset
Remission
PSL + CsA
Case 6
Onset
Non-remission
Remission
CsA
TCZ
Blood collection

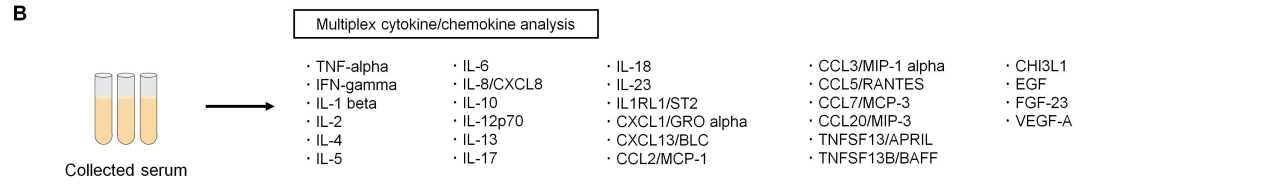
B
Multiplex cytokine/chemokine analysis
Collected serum
・TNF-alpha
・IFN-gamma
・IL-1 beta
・IL-2
・IL-4
・IL-5
・IL-6
・IL-8/CXCL8
・IL-10
・IL-12p70
・IL-13
・IL-17
・IL-18
・IL-23
・IL1RL1/ST2
・CXCL1/GRO alpha
・CXCL13/BLC
・CCL2/MCP-1
・CCL3/MIP-1 alpha
・CCL5/RANTES
・CCL7/MCP-3
・CCL20/MIP-3
・TNFSF13/APRIL
・TNFSF13B/BAFF
・CHI3L1
・EGF
・FGF-23
・VEGF-A

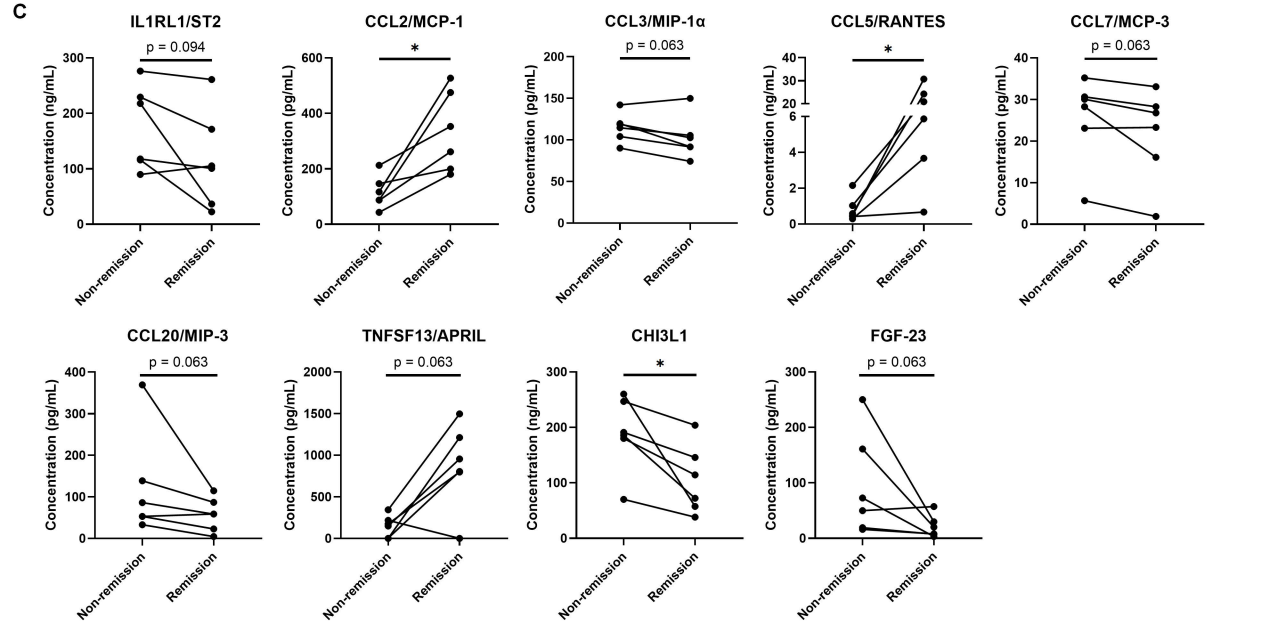
C
IL1RL1/ST2
p = 0.094
CCL2/MCP-1
*
CCL3/MIP-1α
p = 0.063
CCL5/RANTES
*
CCL7/MCP-3
p = 0.063
CCL20/MIP-3
p = 0.063
TNFSF13/APRIL
p = 0.063
CHI3L1
*
FGF-23
p = 0.063
Concentration (ng/mL)
Concentration (pg/mL)
Non-remission
Remission

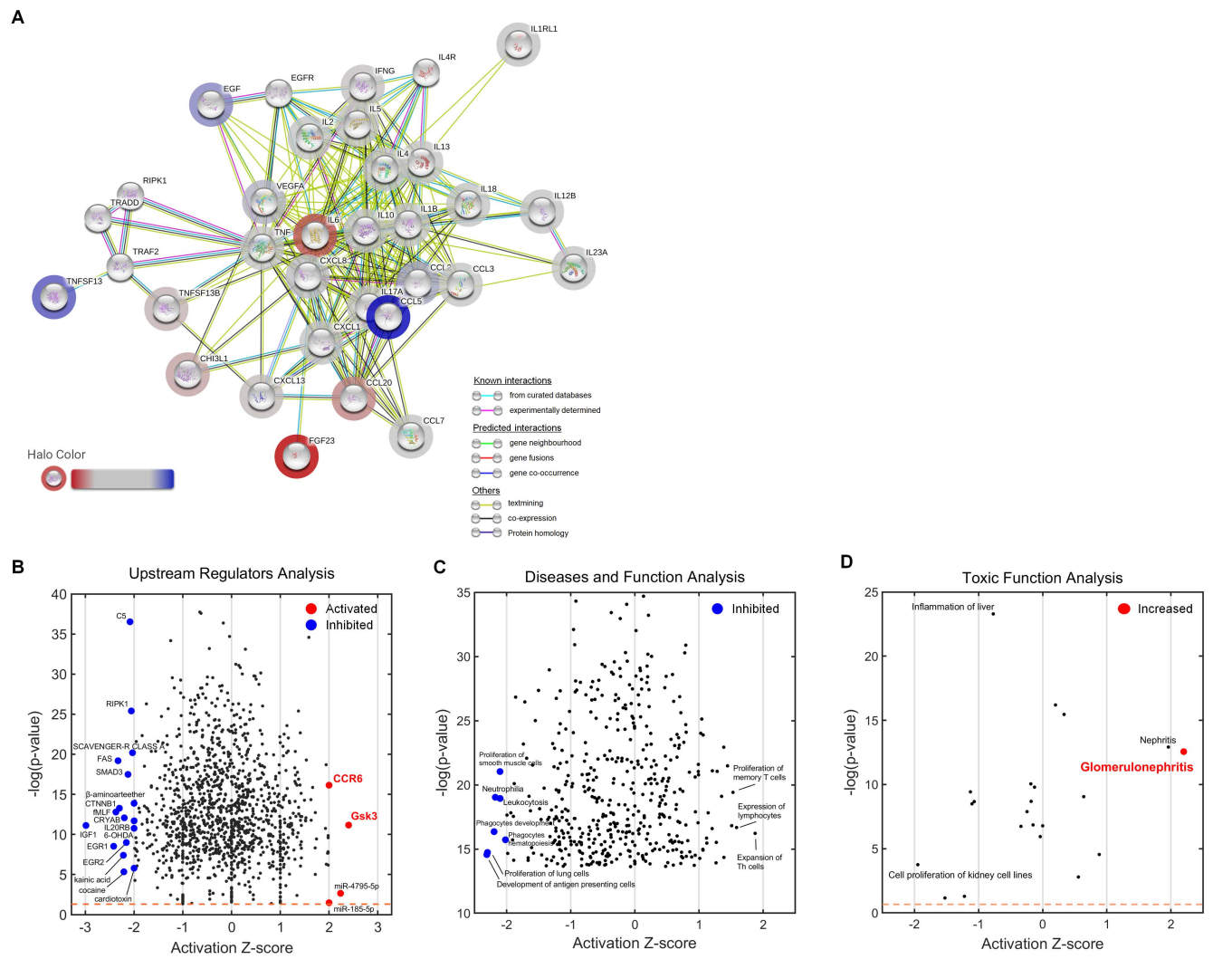
A
IL1RL1
IL4R
IFNG
EGF
EGFR
IL5
IL2
IL13
IL4
RIPK1
VEGFA
IL18
IL12B
TRADD
IL6
IL10
IL1B
TNF
TRAF2
IL23A
CXCL8
CCL4
CCL3
TNFSF13
TNFSF13B
IL17A
CCL5
CXCL1
CHI3L1
CXCL13
CCL20
CCL7
FGF23
Halo Color
Known interactions
from curated databases
experimentally determined
Predicted interactions
gene neighbourhood
gene fusions
gene co-occurrence
Others
textmining
co-expression
Protein homology
B
Upstream Regulators Analysis
Activated
Inhibited
C5
RIPK1
SCAVENGER-R-CLASS-A
FAS
SMAD3
CCR6
β-aminoarteether
CTNNB1
fMLF
CRYAB
Gsk3
IL20RB
IGF1
6-OHDA
EGR1
EGR2
kainic acid
cocaine
cardiotoxin
miR-4795-5p
miR-185-5p
-log(p-value)
Activation Z-score
C
Diseases and Function Analysis
Inhibited
Proliferation of smooth muscle cells
Proliferation of memory T cells
Neutrophilia
Leukocytosis
Expression of lymphocytes
Phagocytes development
Phagocytes
Hematopoiesis
Expansion of Th cells
Proliferation of lung cells
Development of antigen presenting cells
-log(p-value)
Activation Z-score
D
Toxic Function Analysis
Increased
Inflammation of liver
Nephritis
Glomerulonephritis
Cell proliferation of kidney cell lines
-log(p-value)
Activation Z-score

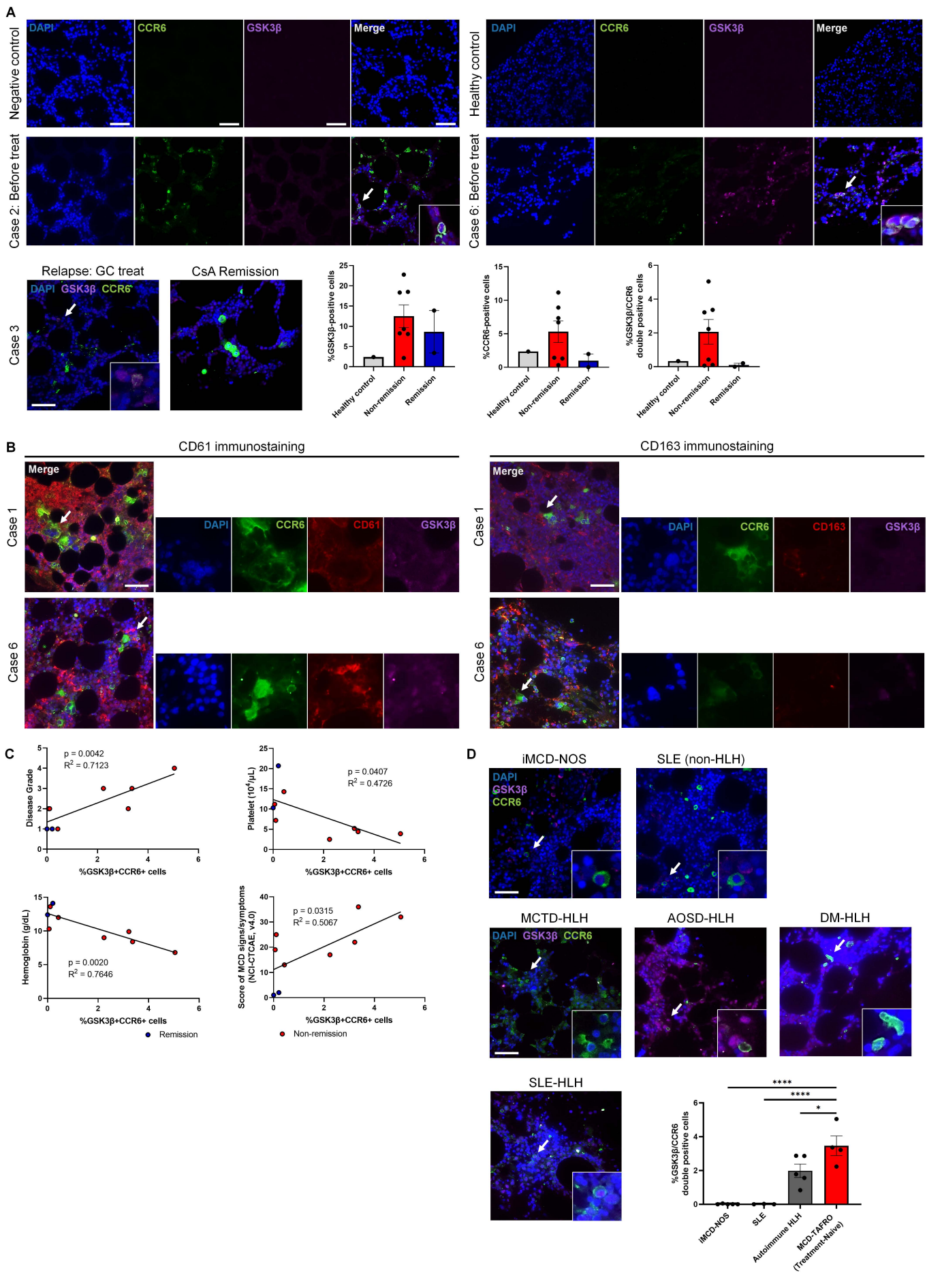
A
Negative control
Healthy control
Case 2: Before treat
Case 6: Before treat
DAPI
CCR6
GSK3β
Merge
Relapse: GC treat
CsA Remission
Case 3
%GSK3β-positive cells
%CCR6-positive cells
%GSK3β/CCR6 double positive cells
Healthy control
Non-remission
Remission
B
CD61 immunostaining
CD163 immunostaining
Case 1
Case 6
CD61
CD163
C
Disease Grade
p = 0.0042
R2 = 0.7123
Platelet (10^4/μL)
p = 0.0407
R2 = 0.4726
Hemoglobin (g/dL)
p = 0.0020
R2 = 0.7646
Score of MCD signs/symptoms (NCI-CTCAE, v4.0)
p = 0.0315
R2 = 0.5067
%GSK3β+CCR6+ cells
Remission
Non-remission
D
iMCD-NOS
SLE (non-HLH)
MCTD-HLH
AOSD-HLH
DM-HLH
SLE-HLH
****
****
*
SLE
Autoimmune HLH
MCD-TAFRO (Treatment-Naive)

SUPPLEMENTAL MATERIALS

Table of Contents:

Supplementary Methods

Diagnosis of multicentric Castleman disease-TAFRO (MCD-TAFRO)

A diagnosis of multicentric Castleman disease-TAFRO (MCD-TAFRO) requires all three major categories and at least two of four minor categories: major categories included anasarca, thrombocytopenia and systemic inflammation, and minor categories included Castleman disease-like features on lymph node biopsy, reticulin myelofibrosis, organomegaly, and progressive renal insufficiency. Exclusion of malignancies, autoimmune disorders, infectious diseases, POEMS (Polyneuropathy, Organomegaly, Endocrinopathy, Monoclonal protein, Skin changes) syndrome, hepatic cirrhosis, and thrombotic thrombocytopenic purpura/haemolytic uremic syndrome is required for a diagnosis of MCD-TAFRO [1].

Case descriptions of six MCD-TAFRO patients

The case 1 is a 48-year-old woman manifesting chronic sicca symptoms with anti-Ro/La antibodies, leading to a diagnosis of primary Sjögren's syndrome (PSS) (Fig. S1A). Because she presented no other manifestations related to SS, she was followed up without treatment. However, eight months after the diagnosis, she developed point-like subcutaneous bleedings. Laboratory findings revealed severe thrombocytopenia and positive anti-Helicobacter pylori antibody. Therefore, she was diagnosed with PSS associated-autoimmune thrombocytopenia and was treated with prednisolone (1.0 mg/kg) along with antibiotic therapy for H. pylori. However, she subsequently manifested high fever and abdominal swelling with pain. Although she was treated with broad-spectrum antibiotics, she showed little improvement. Therefore, she was referred to our hospital. A restudy of the laboratory findings showed elevated serum levels of C-reactive protein (CRP) and renal dysfunction. Computed tomography (CT) demonstrated pleural effusion, ascites, splenomegaly, and mild systemic lymphadenopathy (Fig. S1B). Although dry tap was observed on bone marrow aspiration (BMA), BM biopsy revealed megakaryocytic hyperplasia with mild myelofibrosis (Fig. S1C). We diagnosed the patient with MCD-TAFRO, and administered methylprednisolone pulse therapy, tocilizumab, and thrombopoietin receptor

agonist (TPORA); however, these were ineffective (Fig. S1B). Subsequently, she was treated with rituximab (375 mg/m2/week, four times), and her condition transiently ameliorated. Finally, after the administration of cyclosporine A (CsA), she sustainably recovered (Fig. S1B).

The case 2 is a 47-year-old female farmer manifesting Raynaud's phenomenon (RP) with a positive anti-nuclear antibody and anti-U1 ribonucleoprotein antibody (Fig. S1D) [2]. Because she demonstrated no symptoms associated with systemic lupus erythematosus (SLE), systemic sclerosis, and inflammatory myopathies, she did not meet the diagnostic criteria of mixed connective tissue disease. She was treated only with vasodilators for RP. Seven years later, she developed acute abdominal pain, and the gallbladder wall thickening and stone were detected by ultrasound, leading to the diagnosis of acute cholecystitis. Although she received fasting therapy and antibiotics, she did not achieve an improvement. She subsequently developed fever, dyspnoea, and abdominal distention, and she was transferred to our unit. Laboratory investigations revealed anaemia, thrombocytopenia, hypalbuminaemia, renal failure (serum creatinine 5.4 mg/dL), and systemic inflammation. Hypocomplementemia was not observed. Urinalysis showed haematuria and nephrotic-ranged proteinuria with active urine sediments. CT revealed bilateral pleural effusion, massive ascites, splenomegaly, and slight lymphadenopathy. The patient was initially diagnosed with SLE from the evidence of serositis, nephritis, hematopoietic injury, and positive autoantibodies. Although we administered methylprednisolone pulse therapy followed by prednisolone (1.0 mg/kg), mycophenolate mofetil, and tacrolimus, which is one of calcineurin inhibitors binding FK506 binding protein, with transient haemodialysis, her condition was worsening. We performed BM biopsy for a re-evaluation of the disease state, leading the discovery of mild myelofibrosis with hyperplasia of slightly atypical, multinuclear megakaryocytes. We diagnosed her with MCD-TAFRO. Despite tocilizumab therapy and TPORA, her manifestations did not improve. After the administration of CsA, the patient finally achieved full recovery.

The case 3 is a 64-year-old man presenting with generalized oedema (Fig. S1E). The blood test showed thrombocytopenia, renal impairment, and elevated soluble IL-2 receptor (sIL-2R) level. CT scan demonstrated pleural/peritoneal effusion, abdominal lymphadenopathy. BM biopsy revealed hypercellular marrow with myelofibrosis. He was first diagnosed with autoimmune thrombocytopenia and treated with prednisolone of 60 mg daily, improving his conditions. However, when prednisolone was tapered to 10 mg daily, generalized oedema flared up. Re-examination of laboratory data showed anaemia, thrombocytopenia and mild renal dysfunction. Mild elevated level of serum CRP and interleukin (IL)-6, and marked elevation of plasma vascular endothelial growth factor (VEGF) level were observed. Antinuclear antibody was positive, but the disease-specific autoantibodies were negative. Whole-body CT demonstrated body fluid cavity effusion with hepatosplenomegaly and BM biopsy revealed aggregated megakaryocytes and mild reticulin fibrosis (Fig. S1F). We diagnosed the patient with MCD-TAFRO, and administered methylprednisolone pulse therapy with tacrolimus and intravenous immunoglobulins (IVIg). However, the patient did not respond. We switched tacrolimus to CsA, and then the patient fully recovered. A follow-up of BM biopsy revealed decreases of megakaryocytes and reticulin fibrosis (Fig. S1F).

The case 4 was a 67-year-old woman complaining of fever, cough and oedema resistant with antibiotics (Fig. S1G). Laboratory data showed thrombocytopenia and renal impairment. CT demonstrated anasarca and hepatosplenomegaly. Lymph node biopsy revealed atrophic germinal centres, increased interfollicular vascularity and plasmacytosis like CD-like pathology (Figure 1H). She was diagnosed with MCD-TAFRO. Although he was treated with methylprednisolone pulse therapy, rituximab and tocilizumab, she did not respond to treatment and demonstrated respiratory failure due to massive pleural effusion, requiring mechanical ventilation in the intensive care unit. She recovered after tacrolimus administration. However, the disease flared up when prednisolone was tapered to 12.5 mg daily. Laboratory test demonstrated prominent elevated levels of serum IL-6 and positivity of antinuclear antibody and anti-Ro antibody. CT

scan showed pleural and peritoneal effusion, and hepatosplenomegaly. Although we added a high dose of prednisolone and rituximab on tacrolimus, these drugs did not improve her symptoms. We administered IVIg therapy and switched tacrolimus to CsA, subsequently improving her conditions.

The case 5 was a 62-year-old woman presenting with generalized oedema (Fig. S1J). Laboratory findings showed thrombocytopenia, mild renal dysfunction and positive antiulcer antibody. Urinalysis demonstrated haematuria and nephrotic range proteinuria with active urine sediments. CT showed pleural and peritoneal effusion, and systemic lymphadenopathy. Her symptoms were resistant to levofloxacin treatment. Cervical lymph node biopsy revealed atrophy of the germinal centre and hyaline vascular proliferation with histiocyte infiltration. We diagnosed the patient with MCD-TAFRO and, administered prednisolone (1.0 mg/kg daily) and CsA. The patient subsequently recovered fully.

The case 6 was a 66-year-old woman manifesting with fever and dyspnoea (Fig. S1I). Although she was treated with antibiotics, progressive symptoms including thrombocytopenia, renal insufficiency, mild cervical lymphadenopathy and body cavity fluid collection with hepatosplenomegaly were observed. Urine analysis showed proteinuria and haematuria. Laboratory test demonstrated marked elevation of IL-6 and VEGF level, and positive autoantibodies including rheumatoid factor, antinuclear antibody, anti-double-stranded DNA antibody and anti-Ro antibody. She was diagnosed with MCD-TAFRO. We administered methylprednisolone pulse therapy, continuous intravenous CsA. However, her condition was worsening, and laboratory findings revealed severe microangiopathic haemolytic anaemia with thrombocytopenia, liver/renal failure. We diagnosed the patient with CsA-induced thrombotic microangiopathy. We discontinued CsA and administered tocilizumab and as-needed fresh frozen plasma. Although transient mechanical ventilation for respiratory failure was required, her condition was gradually improved and finally recovered.

References

1. Masaki Y, Kawabata H, Takai K, et al. 2019 Updated diagnostic criteria and disease severity classification for TAFRO syndrome. *Int J Hematol.* 2020;**111**:155-8.
2. Abe N, Fujieda Y, Atsumi T. Diagnosis of Exclusion? A mimicker of serious lupus flare. *The Rheumatologist.* August 12, 2020, 2020: 33-4.

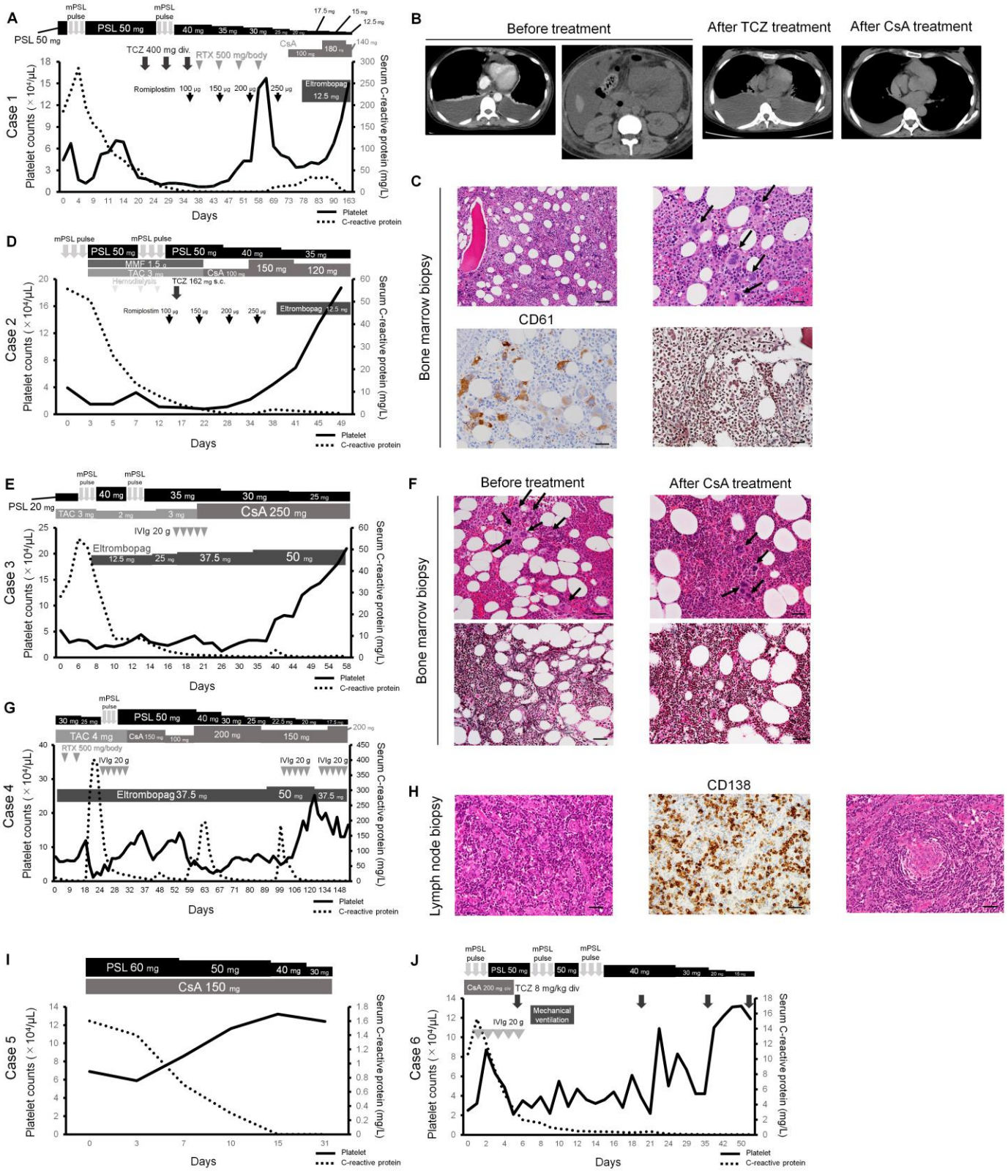

Supplementary Figure S1. Clinical course and relevant data of a multicentric Castleman disease-TAFRO cases in this study

(**A, D, E, G, I** and **J**) Timeline of clinical course and laboratory data of the presented six cases of multicentric Castleman disease-TAFRO (MCD-TAFRO). (**B**) Computed tomography (CT)

findings of the case 1 corresponding to therapeutic course. (**C**) Pathology of bone marrow biopsy in the case 1. (Upper) Arrow indicates megakaryocyte, hematoxylin-eosin staining. (Lower left) CD61 immunostaining, a marker of megakaryocytes. (Lower right) Gitter staining for reticulin fibers. Scale bar, (upper left and lower) 50 μm, (upper right) 20 μm. (**F**) Ameliorating pathology of bone marrow biopsy in the case 2 corresponding to clinical course. (Upper) Arrow indicates megakaryocyte, hematoxylin-eosin staining. (Lower) Gitter staining for reticulin fibers. Scale bar, 50 μm. (**H**) Pathology of lymph node biopsy in the case 4. (Left) Marked infiltration of plasma cells, hematoxylin-eosin staining. (Center) CD138 immunostaining, a marker of plasma cells. (Right) Hyalinization and remarkable vascular proliferation of germinal centers, hematoxylin-eosin staining. Scale bar, (left and right) 50 μm, (center) 20 μm.
Abbreviations: CsA, cyclosporine A; IVIg, intravenous immunoglobulin; MMF, mycophenolate mofetil; mPSL, methylprednisolone; PSL, prednisolone; RTX, rituximab; TAC, tacrolimus, TCZ, tocilizumab.

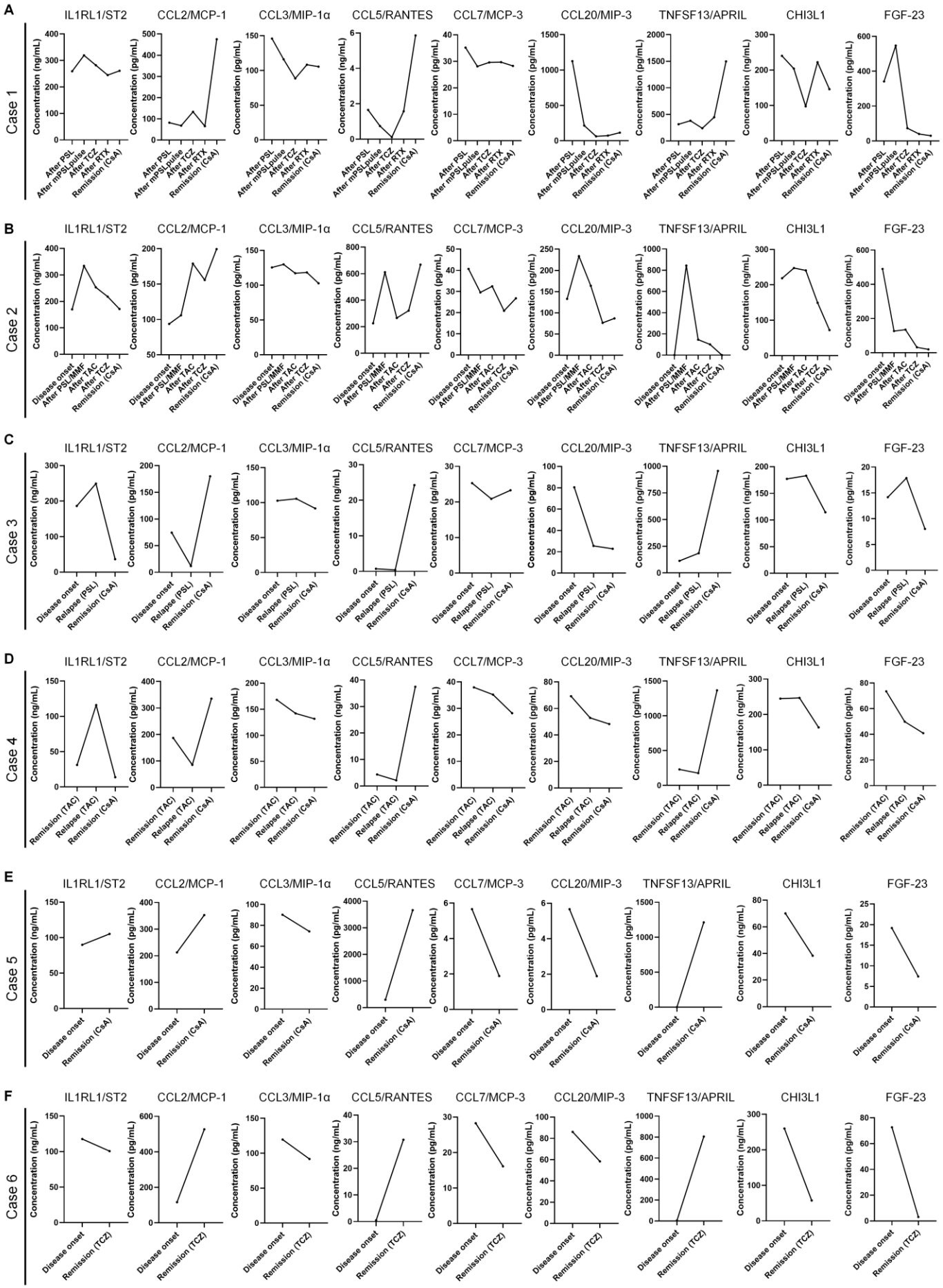
A
Case 1
B
Case 2
C
Case 3
D
Case 4
E
Case 5
F
Case 6
IL1RL1/ST2
CCL2/MCP-1
CCL3/MIP-1α
CCL5/RANTES
CCL7/MCP-3
CCL20/MIP-3
TNFSF13/APRIL
CHI3L1
FGF-23
Concentration (ng/mL)
Concentration (pg/mL)
After PSL
After mPSL/pulse
After PSL/MMF
After TAC
After TCZ
After RTX
Remission (CsA)
Disease onset
Relapse (PSL)
Relapse (TAC)
Remission (TAC)
Remission (TCZ)

Supplementary Figure S2. Changes of the serum cytokine and chemokine levels in the clinical course of the patients with MCD-TAFRO

(**A-E**) Measured values of serum cytokines and chemokine as to therapeutic regimen in the case 1 to 6 with MCD-TAFRO.

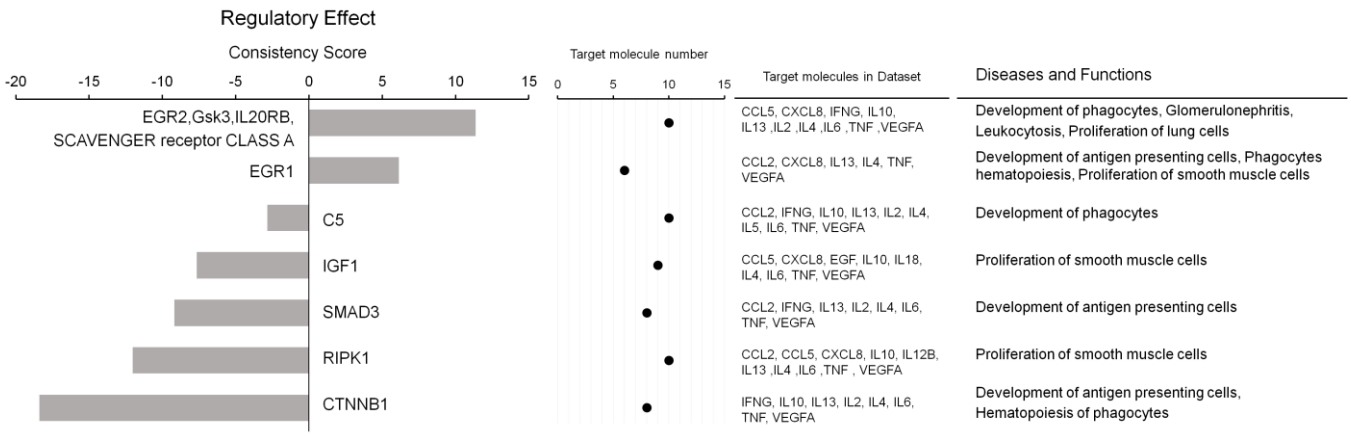

Supplementary Figure S3. Regulator effects analysis of the predicted upstream regulators in Ingenuity Pathway Analysis

Each predicted upstream regulator is described with Consistency Score, which is calculated for each regulator effect network. The higher scores are awarded to networks that are directionally consistent and those means that most of the pathways from the regulators to target molecule (cytokines and chemokine in this case) to disease/function, are consistent with the predicted status of the regulators, the observed direction of the targets' expression in the dataset and the expected effects on the downstream disease and toxic function. Regulator effects analysis were performed by Ingenuity Pathway Analysis.

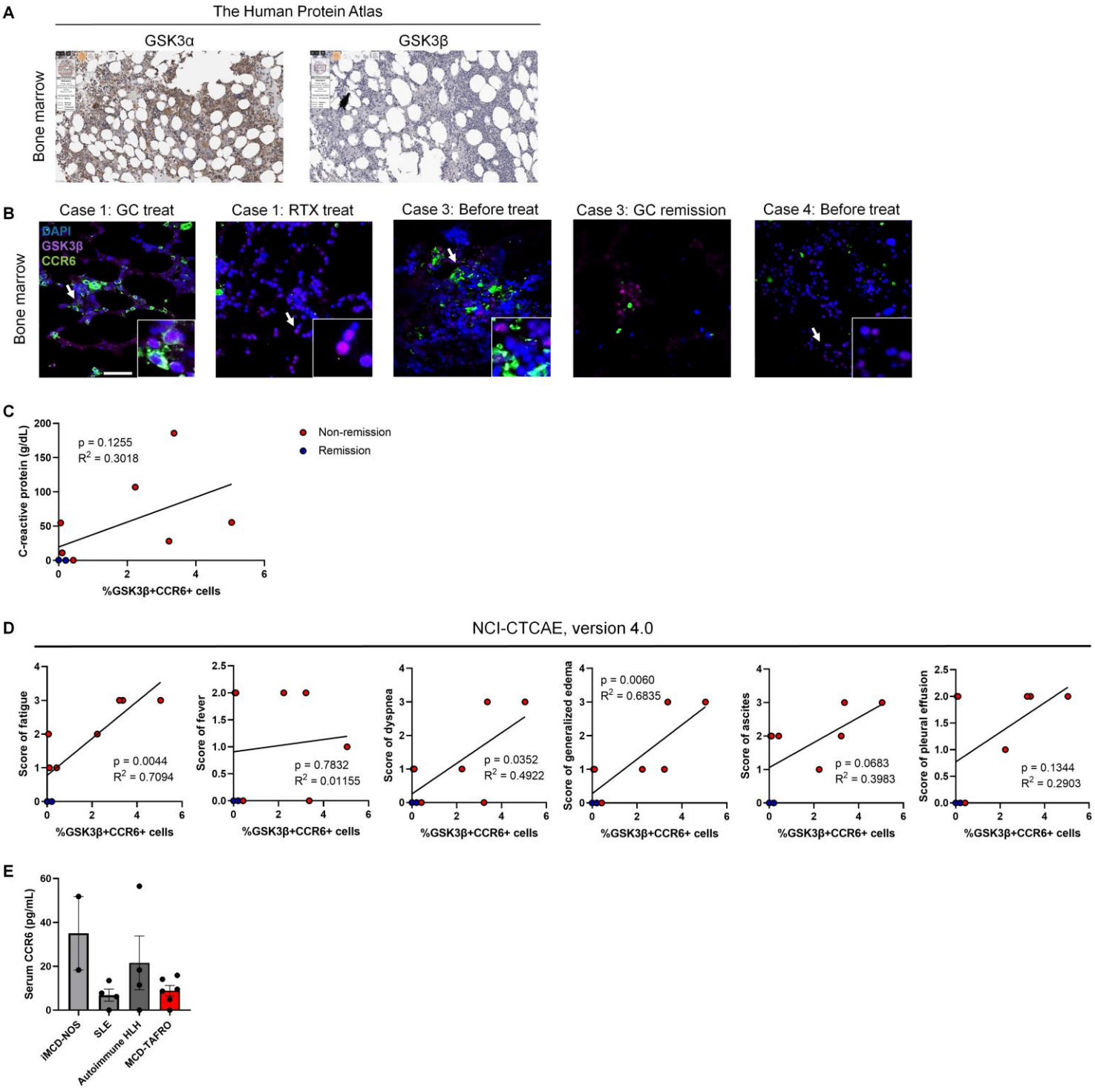

Supplementary Figure S4. Additional images of immunohistochemistry with the correlation analyses between the quantifying result of immunohistochemistry and clinical data

(**A**) Glycogen synthase kinase (GSK) 3α and 3β protein expression in the human bone marrow published in The Human Protein Atlas (http://www.proteinatlas.org). (**B**) Immunohistochemical images of bone marrow overlaid with GSK3β (magenta) and CCR6 (green). The magnified panel

shows the arrow-indicated area. Scale bars, 50 μm. (**C, D**) Additional correlation analyses between GSK3β/CCR6-double-positive cells in bone marrow of MCD-TAFRO patients and their clinical data. Dot plot shows individual cases and blue color indicates the patient with remission state; red with non-remission state. Pearson's product-moment correlation coefficient was used for statistical analysis. (**E**) Serum C-C chemokine receptor (CCR) 6 levels in patients with MCD-not otherwise specified (NOS) (n = 2), systemic lupus erythematosus (SLE) (n = 4) and autoimmune haemophagocytic lymphohistiocytosis (HLH) (n = 4) secondary to mixed connective tissue disease, adult-onset Still's disease, dermatomyositis and MCD-TAFRO (n = 6). ANOVA with post-hoc Holm-Sidak method. Data are mean ± s.e.m.

Supplementary Table S1. Multiplex cytokines/chemokines analysis results in the six MCD-TAFRO patients

Analytes	Case 1		Case 2		Case 3		Case 4		Case 5		Case 6	
	Non-remission	Remission	Non-remission	Remission	Non-remission	Remission	Non-remission	Remission	Non-remission	Remission	Non-remission	Remission
TNF-alpha	2.01	0.06	2.04	3.71	2.10	1.93	1.75	4.41	0.30	0.00	0.00	0.00
IFN-gamma	0.00	0.00	0.00	0.00	0.00	0.00	0.00	0.00	1.93	0.00	0.00	0.00
IL-2	0.05	0.00	0.02	0.00	0.00	0.00	0.00	0.00	0.00	0.00	0.00	0.00
IL-4	2.39	3.96	0.83	2.18	0.75	3.41	3.41	1.12	0.00	4.89	3.66	0.75
IL-5	0.13	0.21	0.15	0.15	0.16	0.11	0.15	0.15	0.18	0.08	0.34	0.15
IL-6	39.91	5.84	12.56	5.18	0.00	0.00	0.00	0.00	3.47	0.00	15.08	21.91
IL-8/CXCL8	17.84	13.32	6.59	6.13	14.39	52.31	21.88	21.59	1.30	9.31	3.97	39.92
IL-10	0.00	0.00	2.35	1.43	0.00	0.00	0.00	0.50	0.00	0.00	0.00	2.10
IL-12p70	0.00	0.00	5.69	0.00	0.00	0.00	395.49	326.73	0.00	0.00	0.00	0.00
IL-13	0.00	0.00	5.33	0.00	6.66	0.00	277.07	332.04	0.00	0.00	13.32	0.00
IL-18	251.62	190.70	215.25	205.57	311.39	175.70	121.75	302.09	87.47	141.40	101.00	211.06
IL1RL1/ST2	276.22	261.03	229.26	171.29	217.83	36.57	115.98	22.50	89.83	105.17	117.73	100.69
CXCL1/GRO alpha	140.74	99.21	63.12	32.69	71.60	233.18	117.65	183.83	0.00	6.30	87.22	98.51
CXCL13/BLC	225.62	309.61	617.99	174.93	1252.88	230.08	848.75	328.23	550.07	210.17	522.61	1188.36

CCL2/MCP-1	87.16	475.24	146.78	199.49	43.13	180.16	85.95	261.44	212.36	352.86	116.66	526.99
CCL3/MIP-1 alpha	114.62	105.46	118.69	102.66	104.06	91.66	142.04	149.86	90.15	74.20	119.64	91.82
CCL5/RANTES	1.03	5.86	0.42	0.67	0.58	24.30	2.16	20.90	0.29	3.66	0.47	30.70
CCL7/MCP-3	30.62	28.25	30.07	26.79	23.09	23.28	35.22	33.07	5.66	1.89	28.25	16.12
CCL20/MIP-3	369.39	114.70	138.69	86.92	52.97	22.85	52.92	58.75	33.10	4.58	86.11	58.38
TNFSF13/APRIL	344.52	1496.30	218.19	0.00	149.14	955.71	175.78	797.97	0.00	1212.14	4.50	804.71
TNFSF13B/BAFF	1760.91	2606.52	1160.43	592.57	1824.83	383.08	942.95	551.86	1020.97	231.15	1233.08	410.91
CHI3L1	190.96	145.88	185.70	72.12	180.02	114.40	246.72	204.05	70.06	38.27	260.03	57.48
EGF	4.19	15.86	0.29	0.00	0.63	108.06	56.78	45.35	0.00	7.94	0.00	18.69
FGF-23	250.20	29.70	160.97	20.07	16.02	8.01	49.85	57.18	19.16	7.42	72.64	3.08
VEGF-A	401.26	823.13	43.49	42.95	112.52	330.16	43.75	12.07	3.84	527.56	46.54	50.00

The concentration unit for IL1R1/ST2, CCL5/RANTES and CHI3L1, ng/mL; the others, pg/mL

The average serum values of cytokines and chemokines corresponding to the disease activity status are described.

Abbreviations: tumor necrosis factor, TNF; interferon, IFN; interleukin, IL; C-X-C motif chemokine ligand, CXCL; IL-1 receptor-like 1, IL1RL1; Growth-related oncogene, GRO; B lymphocyte chemoattractant, BLC; C-C motif chemokine ligand, CCL; monocyte chemotactic protein, MCP; macrophage inflammatory protein, MIP; Regulated on Activation, Normal T cell Expressed and Secreted, RANTES; TNF ligand superfamily member 13, TNFSF13; A proliferation-inducing ligand, APRIL; B cell activating factor belonging to the TNF family, BAFF; Chitinase-3-like-1, CHI3L1; epidermal growth factor, EGF; fibroblast growth factor, FGF-23; vascular endothelial growth factor, VEGF

Supplementary Table S2. Multicentric Castleman's disease signs and symptoms by NCI-CTCAE, v4.0

Type of MCD signs and symptoms	NCI-CTCAE, version 4.0 adverse event
General MCD-related	1. Fatigue
	2. Malaise
	3. Hyperhidrosis
	4. Night sweats
	5. Fever
	6. Weight loss
	7. Anorexia
	8. Tumor pain
	9. Dyspnea
	10. Pruitis
Autoimmune phenomena	11. Autoimmune disorder
	12. Immune system disorder
Fluid retention	13. Generalized edema
	14. Edema face
	15. Edema limbs
	16. Edema trunk
	17. Genital edema

	18. Localized edema
	19. Neck edema
	20. Periorbital edema
	21. Capillary leak syndrome
	22. Ascites
	23. Pleural effusion
	24. Pericardial effusion
Neuropathy	25. Peripheral motor neuropathy
	26. Peripheral sensory neuropathy
	27. Nervous system disorder, other
Skin disorders	28. Rash acneiform
	29. Rash maculo-papular
	30. Papulopustular rash
	31. Purpura
	32. Skin hyperpigmentation
	33. Skin induration
	34. Skin disorder, other

Abbreviations: NCI-CTCAE, v4.0, National Cancer Institute Common Terminology Criteria for Adverse Events version 4.0.